JOC The Journal of Organic Chemistry

Article

pubs.acs.org/joc

Covalent Dimers of 1,3-Diphenylisobenzofuran for Singlet Fission: Synthesis and Electrochemistry

Akin Akdag,[†,‡,∥] Abdul Wahab,[§,⊥] Pavel Beran,[‡] Lubomír Rulíšek,[‡] Paul I. Dron,[†] Jiří Ludvík,*[,§] and Josef Michl*[,†,‡]

[†]Department of Chemistry and Biochemistry, University of Colorado, Boulder, Colorado 80309-0215, United States

[‡]Institute of Organic Chemistry and Biochemistry, Academy of Sciences of the Czech Republic, 16610 Prague 6, Czech Republic

[§]J. Heyrovský Institute of Physical Chemistry, Academy of Sciences of the Czech Republic, Dolejškova 3, 18223 Prague 8, Czech Republic

Supporting Information

ABSTRACT: The synthesis of covalent dimers in which two 1,3-diphenylisobenzofuran units are connected through one phenyl substituent on each is reported. In three of the dimers, the subunits are linked directly, and in three others, they are linked via an alkane chain. A seventh new compound in which two 1,3-diphenylisobenzofuran units share a phenyl substituent is also described. These materials are needed for investigations of the singlet fission process, which promises to increase the efficiency of solar cells. The electrochemical oxidation and reduction of the monomer, two previously known dimers, and the seven new compounds have been examined, and reversible redox potentials have been compared with results obtained from density functional theory. Although the overall agreement is satisfactory, some discrepancies are noted and discussed.

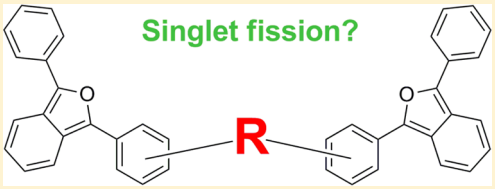

INTRODUCTION

1,3-Diphenylisobenzofuran (**1**, Chart 1) is a long-known and commercially available compound that has seen considerable use for semiquantitative detection of singlet oxygen.[1] It originally elicited our interest because theoretical considerations led to the suggestion[2] that it should be efficient as a model chromophore for singlet fission,[3] a photophysical process in which a singlet excited chromophore shares its energy with a ground-state neighbor and both end up in their excited triplet states. Materials that undergo efficient singlet fission are very rare[4] but are of considerable interest for solar cells, since in principle they permit an increase in maximum theoretical cell efficiency by a factor of ∼1.4.[5] An examination of the photophysics of a thin layer of polycrystalline **1** at a series of temperatures indeed revealed efficient singlet fission.[6−8] Irradiation produced up to two triplet excitations per absorbed photon, implying that both the chromophore itself and the interchromophore coupling in one of the two known modifications of the solid are favorable.[9,10]

Although the high transparency of **1** in most of the visible region of the spectrum[11] and its sensitivity to the combination of air and light preclude any practical use in a solar cell, it is of considerable interest as a model compound in fundamental studies of the still only poorly understood nature of the singlet fission process. One of the issues that is currently most intriguing is the design of efficient interchromophore coupling. This has two aspects, (i) the mutual orientation of the chromophores and (ii) the nature of their covalent attachment, either directly through a single bond or indirectly through a coupling group such as methylene. The approach that others[12,13] and we[14,15] have chosen is to prepare various covalent dimers of chromophores known to undergo singlet fission efficiently as neat solids and to examine their dilute solutions for evidence of singlet fission.

None of the dimers examined so far were efficient. This could be due to a variety of reasons, for instance to the loss of the favorable entropic contribution associated with the ability of the two triplets to diffuse apart in a crystal. One likely reason is apparent upon inspection of the approximate theoretical expressions[3,4] for the interchromophore coupling strengths. According to these formulas, both contributing components, the minor direct path and the major path mediated by virtual charge-transfer states, should be inefficient when the coupling is linear, as it has been in all dimers examined so far. The theory suggests that slip-stacking the chromophores will be much more favorable and, indeed, will be the best arrangement among those considered up to now.

The first two covalent dimers of **1** that were synthesized and tested, **2** and **3**, were linear. They exhibited no detectable singlet fission in solutions in nonpolar solvents, but triplet formation was observed in small yields up to ∼10% in polar solvents, where it proceeded through an observable intramolecular charge-transfer state.[10,14,15] It is not clear whether each charge-transfer excited molecule produced two triplets in a second phase of two-phase singlet fission or just one triplet by ordinary intersystem crossing. In any event, the observation has drawn attention to the possible importance of two-step singlet

Received: August 30, 2014
Published: November 10, 2014

   dx.doi.org/10.1021/jo502004r | J. Org. Chem. 2015, 80, 80−89

Chart 1. Structures 1−10

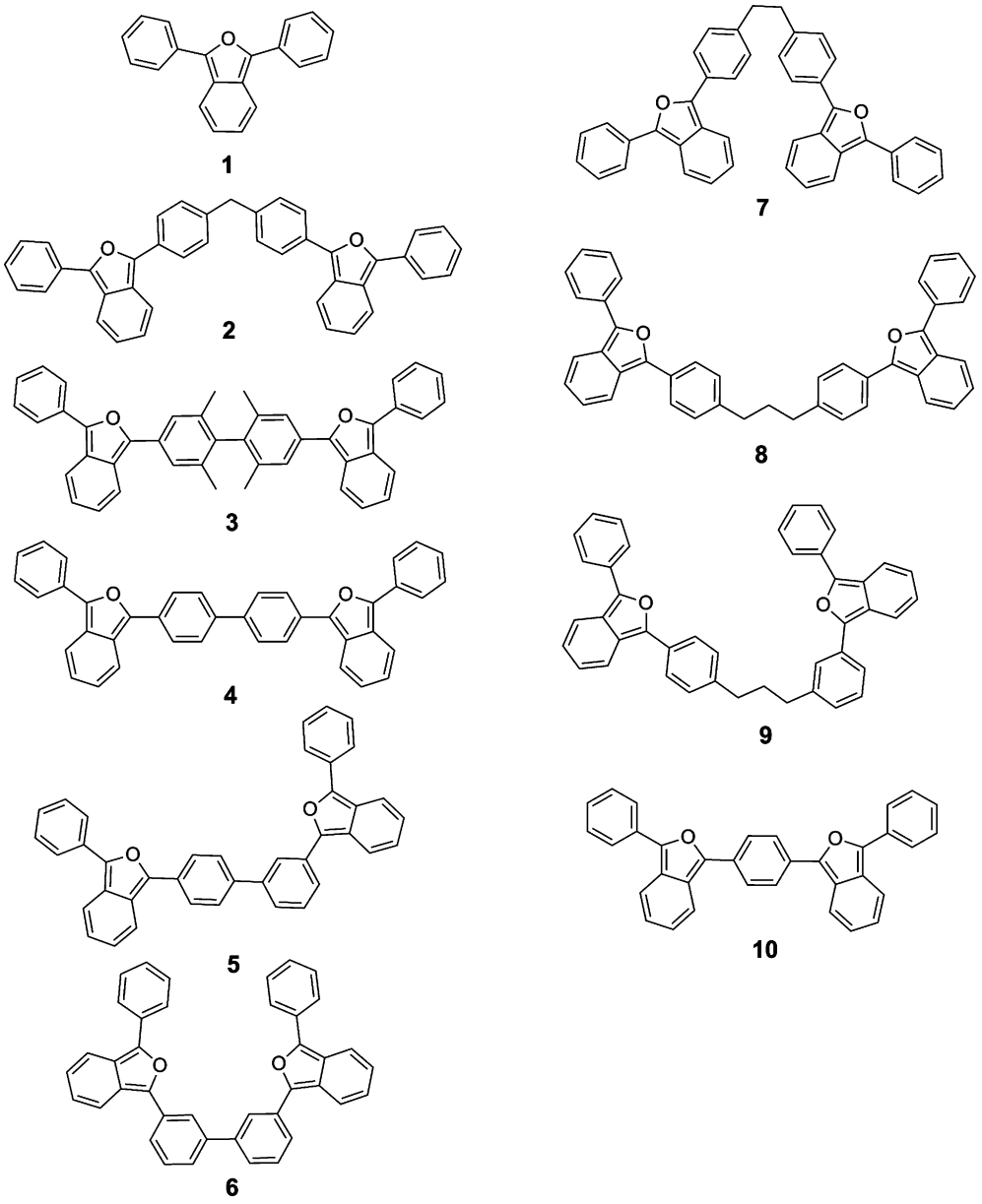

Scheme 1. Preparation of Covalent Dimers

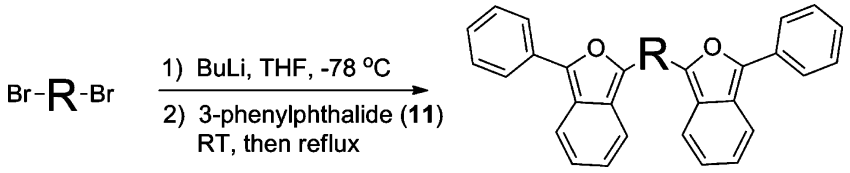

fission. The investigation of **2** and **3** clearly needs to be complemented by an examination of a larger selection of covalent dimers of **1**. Presently, we report the synthesis of compounds **4**−**10**, designed to test both the effects of the choice of the covalent link (**4**−**6**) and the effects of conformational mobility that would permit stacking (**7**−**9**). The related double isobenzofuran **10**, which is not a true dimer of **1**, was added to the series for comparison.

Since the redox properties of potential singlet fission molecules would be critical for their use in solar cells, we have examined the electrochemistry of the monomer and the dimers, both experimentally and computationally. The electrochemical behavior of **10** is quite distinct, and this compound requires a more detailed examination, the results of which will be reported separately.

RESULTS

Synthesis. The preparation of dimers **2** and **3** was described elsewhere.[15] The dimers **4**−**9** were prepared by the addition of a solution of a dilithiated linker compound, prepared from a

dx.doi.org/10.1021/jo502004r | J. Org. Chem. 2015, 80, 80−89

Scheme 2. Synthesis of Linker Compounds

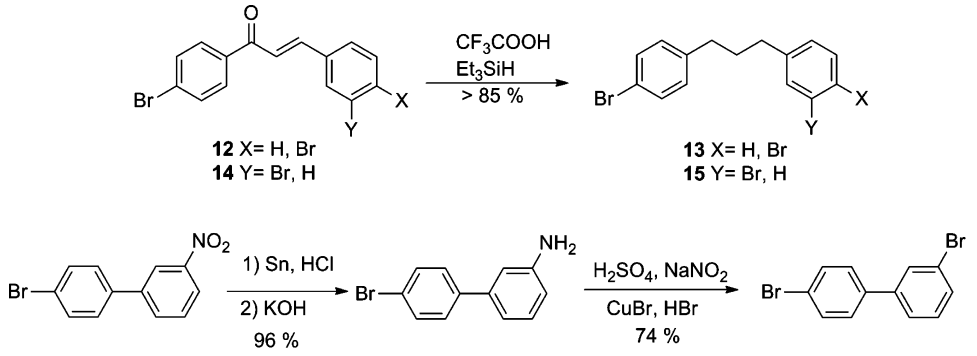

dibromo precursor, to a solution of 3-phenylphthalide (**11**, Scheme 1). Inverse addition did not yield the desired products.

Some of the required linker compounds were known,[16,17] and the routes used to prepare the new ones are shown in Scheme 2.

The precursors for dimers **8** and **9** were synthesized in the same fashion (Scheme 2).[18,19] A condensation of 4-bromoacetophenone with 4-bromobenzaldehyde or 3-bromobenzaldehyde in the presence of sodium ethoxide yielded excellent yields of **12** and **14**. Their catalytic hydrogenation (H_2, Pd/C, 1 atm) produced 1,3-diphenylpropane, but **13** and **15** were obtained by reduction with triethylsilane in trifluoroacetic acid.[20] Reduction of the nitro group in 4′-bromo-3-nitro-1,1′-biphenyl[21] to the amine followed by the Sandmayer reaction afforded 3,4′-dibromo-1,1′-biphenyl.

The general method gave only traces of **10**, and a two-step procedure was used instead, where 1-(4-bromophenyl)-3-phenylisobenzofuran[22] was lithiated and treated with **11** to yield **10**.

Electrochemistry. Direct current polarography and cyclic voltammetry (CV) of **1**−**10** were performed on mercury (reduction) and platinum (oxidation) electrodes in *N*,*N*-dimethylformamide (DMF). Oxidation on a platinum electrode was also examined in acetonitrile at room temperature and in liquid SO_2 at several temperatures from −70 to 22 °C (**4** was very slightly soluble in liquid SO_2 and only at the higher temperatures).

For reduction processes on a hanging mercury drop electrode (HMDE) and in polarographic measurements, the number of electrons involved was determined from the relative height of normalized currents and comparison with *p*-nitrotoluene, which gives a clean reversible one-electron reduction. The number of electrons involved in anodic processes was determined by comparison of normalized peak currents with that of ferrocene, which undergoes a reversible one-electron oxidation. Judging by concentration and scan rate dependence, all oxidation and reduction processes were diffusion-controlled, except that **3** showed an adsorption prewave in CV and polarography, as discussed below.

Oxidation. Cyclic voltammograms were measured in liquid SO_2 (at 0.08−5 V/s and at −70 to 22 °C), in acetonitrile (5.0 V/s), and in DMF (0.2 V/s). In liquid SO_2 containing Oct_4NClO_4, the monomer **1** and two of the dimers (**2**, **4**) undergo oxidation that is completely reversible above 0 °C (Figure 1, Table 1). Their peak current ratios are close to unity and the peak separations are comparable to that of the Fc^+/Fc couple under the same experimental conditions (66 mV for **1**). Clean reversibility was not observed in the absence of a

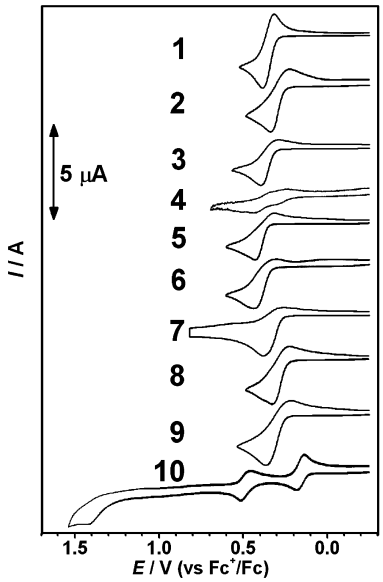

Figure 1. Cyclic voltammograms of **1**−**10** in liquid SO_2 (Pt electrode, 0.1 V/s, 0.1 M Oct_4NClO_4, vs Fc^+/Fc, at 15 °C). Sample concentrations were (4.5 ± 1.0) × 10^{-4} M, except for **4**, where it was lower because of very poor solubility.

Table 1. CV Data for Oxidation of 1−10 in Liquid SO_2 Measured vs Fc^+/Fc (at 15 °C, 0.1 V/s) and in Acetonitrile Measured vs SCE (room temperature, 5.0 V/s) at a Pt Stationary Disk Electrode

	liquid SO_2		acetonitrile
compd	$E_{1/2}$ (vs Fc^+/Fc)[a]	$E_{1/2}$ vs SCE[b]	E_{pa} vs SCE
1	0.35 (67)	0.855	0.88
2	0.28 (112)	0.785	0.78
3	0.34 (106)	0.845	0.82
4	0.27 (60), 0.38 (92)	0.775, 0.885	0.91
5	0.33 (113)	0.835	0.87
6	0.37 (130)	0.875	0.88
7	0.32 (119)	0.825	0.81
8	0.27 (101)	0.775	0.78
9	0.29 (143)	0.795	0.75
10	0.16 (46), 0.48 (58)	0.665; 0.985	0.49[c,d]

[a] $E_{ox} = (E_{pa} + E_{pc})/2$; measured data vs Fc/Fc^+. Values in parentheses are anodic/cathodic peak separations ΔE_p in mV. [b] E_{ox} recalculated vs SCE: $E_{SCE} - E_{Fc/Fc^+}$ = 505 mV (average experimental value of the difference). [c] Poorly defined peak. [d] Compound **10** has an additional irreversible oxidation peak at 1.43 V in liquid SO_2 and at 0.85 in acetonitrile.

dx.doi.org/10.1021/jo502004r | J. Org. Chem. 2015, 80, 80−89

perchlorate salt. The oxidation behavior of the other dimers is quasireversible: their cathodic/anodic peak current ratio is much lower than one and the peak separation is 100−150 mV. For **4**, two reversible one-electron oxidations are observed at 0.27 and 0.38 V vs ferricenium/ferrocene (Fc^+/Fc) (shown in more detail in the Supporting Information, Figure 1S). Similarly, **10** is oxidized in two reversible one-electron processes with peak separations of 46 and 58 mV. Figure 2 shows the noteworthy "inverted" temperature dependence of reversibility for **1** at 0.1 V/s.

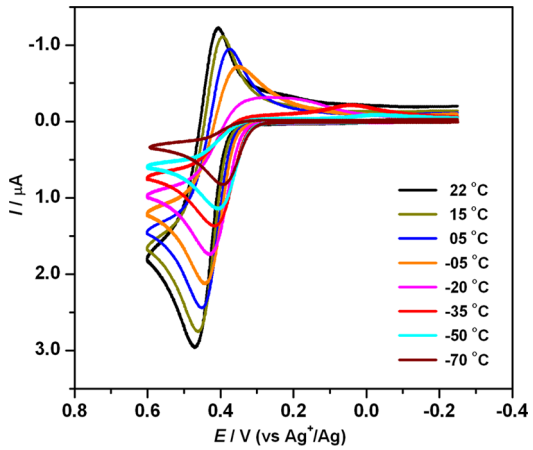

Figure 2. Temperature dependence of cyclic voltammograms of **1** in liquid SO_2 (Pt electrode, 0.1 V/s, 0.1 M Oct_4NClO_4, vs Ag^+/Ag).

In DMF (Figure 3) and in acetonitrile all oxidations are irreversible at the available scan rates (0.05−5.0 V/s) at room temperature, presumably due to a reaction of the primary products with the solvent. The parent **1** exhibits a single irreversible oxidation wave in both solvents. However, at −70 °C and a high scan rate (5.0 V/s), it appears to show a vague

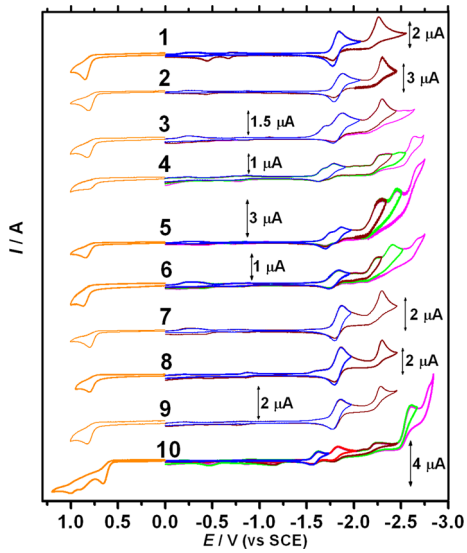

Figure 3. Cyclic voltammograms of **1**−**10** in DMF (0.2 V/s, 0.1 M Bu4NPF6, vs SCE, at room temperature). Sample concentrations were (3.5 ± 1.0) × 10^{-4} M. Reductions were at a hanging mercury drop electrode (HMDE) and oxidations were at a Pt disk electrode (therefore the current cannot be on the same scale; the scale shown applies to the cathodic waves).

cathodic return peak, indicating some reversibility. This is especially true in DMF, although at this temperature the solution is a semitransparent semisolid (melt). Except for **4**, the dimers all exhibit a single oxidation wave in DMF and acetonitrile at a potential close to that of **1**. This appears to be a two-electron process, although the normalized peak currents of the dimers are less than double those of **1**. In DMF, **4** exhibits two very weak, probably one-electron processes at 0.82 and 0.88 V (vs SCE), and **10** displays three irreversible anodic oxidation peaks. In acetonitrile, these processes occur at similar potentials, but they are not well defined.

The oxidation potentials obtained at the same scan rate in liquid SO_2, acetonitrile, and DMF using different reference electrodes are mutually consistent within ±0.04 V (cf. the three sets of measured oxidation potentials in Tables 1 and 2).

Reduction. Typical voltammograms recorded at 0.2 V/s are shown in Figure 3, and the results are summarized in Table 2. The parent **1** undergoes a reversible one-electron reduction at −1.81 V followed by a quasireversible one-electron reduction at −2.28 V. No other reduction peak was found up to the discharge at −2.90 V. The quasireversibility of the second reduction step is manifested at a lower temperature (−20 °C) and a higher scan rate (5.0 V/s) by the appearance of a small anodic counterpeak (Figure 4). When the switching potential is set only a little more negative than the first reduction peak, its full reversibility is observed even at room temperature (Figure 3). However, when it is set a little more negative than the second reduction peak, the anodic counterpeak of the first reversible couple becomes smaller.

The reduction of the dimers **2**, **3**, and **7**−**9** is very similar to that of the monomer **1** (Table 2). In cyclic voltammograms, a single reversible one-electron redox couple at −1.81 to −1.84 V is followed by another reduction peak at −2.29 to −2.31 V, which is irreversible. The normalized current of all reduction processes in the dimers is less than twice that of the monomer **1**. In polarograms, and more clearly in cyclic voltammograms, **3** shows a weak prewave at −1.71 V, attributed to adsorption of the first reduced species, the radical anion of **3**.

The cyclic voltammograms of the dimers **4**−**6** present more complicated reduction patterns: each of these dimers undergoes two successive reversible one-electron reductions, $E(1)$ and $E(2)$, followed by two irreversible reduction steps, $E(3)$ and $E(4)$ (Figure 3, Table 2). Another irreversible reduction peak appears at more negative potentials [∼ −2.67 V, $E(5)$]. The corresponding polarographic curve possesses an approximately two-electron height.

Like its oxidation, the reduction of **10** is easier than those of **1**−**9**. Two successive, reversible one-electron reductions occur at −1.62 and −1.83 V and are followed by two irreversible reductions at −2.24 and −2.61 V. The second irreversible reduction at −2.61 V appears to involve more than two electrons. At even more negative potentials (−2.81 V), another reduction takes place.

Calculations. Since single bonds between aromatic rings are typically twisted by 20°−40°, conformational flexibility provides a considerable challenge to the calculation of the oxidation and reduction potentials of the isobenzofurans **1**−**10**. In **1**−**6** and **10**, the existence of choices for the relative sense of these twists is responsible for the presence of two conformers even for the monomer **1**[11] and for the larger number of conformers of the dimers. In **7**−**9**, the situation is further complicated by additional conformational isomerism in the saturated chain that connects the two isobenzofurans. In the

dx.doi.org/10.1021/jo502004r | J. Org. Chem. 2015, 80, 80−89

Table 2. CV Data for Oxidation (E_{pa}) and Reduction (E_{pc}) of 1−10 in DMF (0.2 V/s) Measured vs SCE[a]

compd	E_{pa}	$E_{pc}(1)$[b]	$E_{pc}(2)$[b]	$E_{pc}(3)$	$E_{pc}(4)$	$E_{pc}(5)$
1	0.85	−1.84 (65)		−2.26		
2	0.81	−1.88 (90)		−2.31		
3	0.82	−1.89 (98)		−2.31		
4	0.82, 0.88	−1.69 (57)	−1.79 (61)	−2.35	−2.49	−2.65
5	0.84	−1.77 (65)	−1.87 (60)	−2.29	−2.45	−2.67
6	0.87		−1.84 (103)[c]	−2.26	−2.41	−2.69
7	0.80	−1.88 (75)		−2.30		
8	0.80	−1.87 (66)		−2.30		
9	0.83	−1.86 (80)		−2.29		
10	0.66, 0.91, 1.00	−1.62 (66)	−1.83 (66)	−2.24	−2.61	−2.81

[a]Oxidation was at a Pt stationary disk electrode and reduction at a HMDE. [b]Values in parentheses are anodic/cathodic peak separations ΔE_p in mV of reversible couples. [c]Broad cathodic and anodic peaks most probably contain two very close reversible couples.

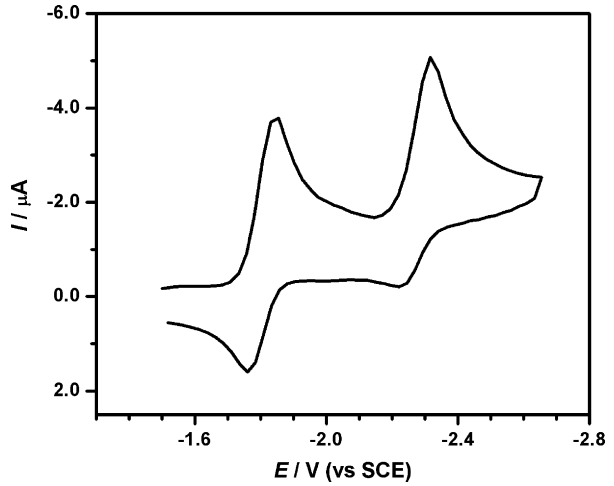

Figure 4. Cyclic voltammogram of 6.5×10^{-4} M **1** in DMF at −20 °C (HMDE, 5.0 V/s, 0.1 M Bu_4NPF_6, vs SCE).

study of electrochemical properties, it also needs to be considered that conformational isomerism may be different in neutral, oxidized, and reduced molecules.

Fortunately, conformers differing only in the relative sense of twist about single bonds between aromatic rings can be expected to exhibit only minute differences in oxidation−reduction and most other properties. This has been established in the case of **1**, where the only observed differentiating feature between the conrotatory and disrotatory conformation is a small difference in the shape of the vibrational envelope of the first electronic absorption band.[11] We have verified this expectation further by locating all 32 conformational minima in the ground states of each of the dimers **4**−**6** and found that their calculated highest occupied molecular orbital (HOMO from DFT) and lowest unoccupied molecular orbital (LUMO from DFT) energies are identical within 0.01 eV.[23] In the present work, we considered 10 conformers for each compound, spanning the conformational space corresponding to rotation about single bonds linking the two monomers. The lowest energy conformer of the neutral, the oxidized, and the reduced forms was used for the calculation of reduction potentials. The molecular geometries of the lowest energy conformers can be found in the Supporting Information.

According to PBE+D3/def2-TZVP energies calculated for **7**, **8**, and **9**, the stacked conformers are favored by 3, 9, and 10 kcal mol^{-1}, respectively. However, we expect the extended conformers to be favored by the entropic term in the expression for free energy by 4−6 kcal.mol^{-1}, as estimated from the $\Delta(E_{ZPVE} - RT \ln Q)$ term (Supporting Information), and we find that they are also favored by COSMO-RS solvation energies, by amounts ranging from ∼4 to ∼7 kcal mol^{-1}. Therefore, we expect only the extended conformer to be present in the solvents used. This expectation is in line with the finding that the computed reduction potentials agree better with the observed ones when extended conformations are used for **7**−**9**.

The calculated oxidation and reduction potentials are collected in Table 3 together with the individual terms (solvation energies, ionization energies, zero-point energy, and the in-vacuum entropic and thermal contributions).

DISCUSSION

The synthesis of the dimeric isobenzofurans **2**−**10** by a single-step double coupling proceeded smoothly with the sole exception of the synthesis of **10**, which had to be prepared in two separate coupling steps. It provided access to a series of compounds suitable for investigations of singlet fission, some of which have already yielded results.[23] The other aspect of the present study, gaining knowledge of the redox potentials of **1** and its dimers, is also of immediate interest in our studies of the photophysics of compounds containing the 1,3-diphenylisobenzofuran chromophore, since intramolecular excited state charge transfer can represent a serious competitor to the desired singlet fission event. The redox potentials will be ultimately relevant for the choice of materials into which an electron or a hole will need to be injected if they are to be tested in solar cells.

Oxidation and Reduction of the Monomer 1. The UV−visible absorption spectra of the radical ions of **1** have been measured using pulse radiolysis and interpreted,[11] but the redox potentials were unknown.

We find that the oxidation of **1** is relatively easy and in liquid SO_2 occurs by a reversible one-electron transfer only about 0.35 V above the oxidation potential of ferrocene. The resulting radical cation is fairly stable. The unusual temperature dependence of reversibility presented in Figure 2 invites additional study. In DMF and acetonitrile, the situation is more complicated in that the oxidation current corresponds to an irreversible two-electron process, based on comparison with the one-electron standard, ferrocene. The primary radical cation undergoes a fast follow-up chemical reaction, most likely with the solvent, and then a second electron transfer occurs (ECEC mechanism). The follow-up reaction is probably suppressed at

dx.doi.org/10.1021/jo502004r | J. Org. Chem. 2015, 80, 80−89

Table 3. Calculated Oxidation and Reduction Potentials of 1−10[a]

compd	IE[b]/eV	$\Delta\Delta G_{gp}$[c]/eV	$\Delta\Delta G_{solv}$[d]/eV	SO_2 E^0_{calcd}/V[e]	SO_2 $E^0_{1/2\ exp}$/V	DMF E^0_{calcd}/V[f]	DMF[g] $E^0_{pa\ exp}$/V
				1e⁻ Oxidation			
1	6.38	0.01	−1.28	0.57 (0.95)	0.85	0.58	0.85
2	5.72	0.01	−0.82	0.36 (0.74)	0.78	0.38	0.81
3	5.71	−0.02	−0.78	0.37 (0.75)	0.84	0.39	0.82
4	5.64	0.00	−0.84	0.27 (0.65)	0.77	0.28	0.82, 0.88
5	5.81	0.02	−0.85	0.43 (0.81)	0.83	0.45	0.84
6	5.93	0.00	−0.92	0.47 (0.85)	0.87	0.49	0.87
7	5.68	0.01	−0.78	0.37 (0.75)	0.82	0.39	0.80
8	5.65	0.02	−0.76	0.36 (0.74)	0.77	0.38	0.80
9	5.70	0.07	−0.76	0.47 (0.85)	0.79	0.49	0.83
10	5.68	0.00	−0.95	0.19 (0.57)	0.66	0.20	0.66
				1e⁻ Reduction			
1	0.99	0.15	1.73			−1.66 (−1.96)	−1.84
2	1.53	0.13	1.33			−1.53 (−1.83)	−1.88
3	1.50	0.17	1.32			−1.53 (−1.83)	−1.89
4	1.72	0.11	1.32			−1.35 (−1.65)	−1.69
5	1.55	0.13	1.36			−1.49 (−1.79)	−1.77
6	1.46	0.17	1.42			−1.48 (−1.78)	−1.84
7	1.58	0.14	1.26			−1.54 (−1.84)	−1.88
8	1.56	0.14	1.19			−1.64 (−1.94)	−1.87
9	1.54	0.08	1.28			−1.62 (−1.92)	−1.86
10	1.62	0.13	1.43			−1.34 (−1.64)	−1.62

[a]All values are in eV or V; potentials are against the SCE (+0.2444 V vs NHE) in DMF and acetone (mimic of SO_2 solvent). See Computational Details, eqs 1 and 2. [b]Adiabatic ionization energies or electron affinities calculated in a vacuum at the PBE+D3/def2-TZVP//PBE-def2-SVP level. [c]The difference in gas-phase chemical potential (including ZPVE) calculated at the PBE+D3/def2-SVP level. [d]The difference in solvation energies between the oxidized and reduced forms, calculated using the COSMO-RS method. [e]In parentheses, values increased by a constant shift of +0.38 V. [f]In parentheses, values reduced by a constant shift of -0.30 V. [g]Oxidations in DMF are irreversible.

low temperatures, and therefore, at high scan rates partial reversibility is observed.

The reduction of **1** is a relatively difficult reversible one-electron process, 2.1 V below the reduction of ferricenium. The electrochemical reduction mechanism of **1** is apparently of the EEC type:

$$\mathbf{1} + e^- \rightarrow \mathbf{1}^{-\bullet} \quad E_1(\text{rev})$$

$$\mathbf{1}^{-\bullet} + e^- \rightarrow \mathbf{1}^{2-} \quad E_2(\text{quasirev})$$

$$\mathbf{1}^{2-} + H^+ \rightarrow \text{products}$$

Quantum chemical calculations of oxidation−reduction potentials are becoming a standard tool complementing experimental data[24−29] and can be helpful for the interpretation of reversible redox behavior. Since reversible potentials are available for **1**, both for oxidation in liquid SO_2 and for reduction in DMF, a meaningful absolute calculation of both potentials versus SCE is possible, using the latest value[27] E^0_{abs}(NHE) = 4.281 V for the absolute potential of the normal hydrogen electrode NHE and the standard value 0.2444 V for the potential of SCE vs NHE. The oxidation potential of **1** is 0.35 V measured against Fc/Fc^+ (Table 1) and 0.85 V after conversion to SCE as a reference, using the measured difference of 0.505 V between the two reference electrodes (cf. the calculated[30] difference of 0.516 V in acetonitrile). The reduction potential is −1.84 V measured against SCE (Table 2). The experimental values relative to the SCE, 0.85 and −1.84 V, can be compared with the absolute computed values converted to SCE, 0.57 and −1.66 V, respectively (Table 3).

Thus, the value computed for the oxidation process is insufficiently positive by ∼0.3 V, and the value computed for the reduction process is insufficiently negative by ∼0.2 V. This is not a very impressive agreement, and the most likely culprits are errors in (i) the COSMO-RS calculation of absolute solvation energies and (ii) the calculation of ionization and electron attachment energies. It is also likely that acetone is only an imperfect mimic for liquid SO_2 in this type of calculation, but parameters for the latter are not available. Admittedly, absolute calculations of redox potentials are difficult, and one can hope for better agreement when comparing the calculated redox potentials within a series of related compounds.

Oxidation and Reduction of Dimers 2−9. The observed oxidation as well as reduction potentials generally differ only little from those of the monomer **1**, placing considerable demands on computational interpretations. With the exception of the reduction of **4**−**6**, the oxidation and the reduction of the dimers occur in one single electrochemical step, suggesting that they proceed on both isobenzofuran units independently at the same potential. The effect of intramolecular electronic communication between the two π systems through the bridge is negligible. Apparently, the saturated alkane bridges in **2**, **7**, **8**, and **9** prevent electron delocalization, as does the perpendicular orientation of the two benzene rings in **3**, imposed by the *o*-methyl substituents. In these cases, the reduction response is analogous to that of **1**, but with twice the current.

The situation is different in the reduction of the directly conjugated compounds **4**−**6**. Instead of two two-electron reduction peaks, as in **2**, **3**, and **7**−**9**, two pairs of one-electron reductions are observed, as each electron transfer that increases the negative charge impedes the next reduction step. This separation of individual reduction steps shows that in this case

dx.doi.org/10.1021/jo502004r | J. Org. Chem. 2015, 80, 80−89

the effect of electronic communication between the two isobenzofuran units is significant.

Not surprisingly, in view of the shape of the frontier molecular orbitals of **1**,[11] the extent of interaction between the two halves in the dimers increases in the order **6** < **5** < **4**. The optimized computed structures of the radical anions of **4**−**6** are more planar than the neutral parent compounds. This is reflected in an equal difference between $E(3)$ and $E(4)$ in all three dimers. The most negative reduction process $E(5)$, observed only in the case of **4**−**6**, is probably due to the biphenylene bridges, which become noninnocent and reducible (cf. Table 2). The origin of the irreversibility of the second reduction processes in all the dimers is probably the high basicity of the resulting tetraanions, which allows them to abstract a proton from the solvent.

The location and the nature of the covalent bridging unit in the dimers **2**−**9** have a remarkably small effect on the oxidation potentials in both DMF and liquid SO_2, which differ from that of **1** by at most 80 mV. The 40−60 mV easier oxidation of **7**−**9** relative to **1** is not likely to be all due to the electron donor effect of the alkane bridge, since the redox potentials of **1** and **3** are nearly identical. This argument is weakened by the location of the methyl groups in the latter in the poorly conjugating meta positions, but it nevertheless appears likely that the slightly easier oxidation of **7**−**9** reflects a stacking stabilization of their radical cations. The limiting currents observed for the oxidation of the dimers are less than twice that of **1**, undoubtedly partially due to their smaller diffusion coefficients, but probably at least in part due to an increased fouling of the electrode. The current response observed for **6** and **7** is even smaller because of their poor solubility.

The reduction potentials within the series **2**−**9** vary only slightly more, within about 200 mV, and are again all roughly equal to that of **1**. As might be expected, the best conjugated dimer **4** is the easiest to reduce.

A comparison with calculations is somewhat less reliable than was the case for **1**, since even in liquid SO_2 only the oxidation of **2**, **4**, and **10** is fully reversible, and the others are only quasireversible. The reductions are all reversible. The calculations correctly predict little variation within the series, but exaggerate it slightly, both for oxidation and for reduction potentials. An empirical adjustment of the calculated values by a constant shift improves the agreement in both cases and reduces the typical discrepancy to less than 0.1 V (Table 3).

In contrast, it is probably significant that the calculations of both oxidation and reduction potentials fail to reproduce the difference between the dimers and the monomer **1**. They predict the dimers to be 0.1−0.3 V easier to oxidize and to reduce than the monomer, and the observed differences are much smaller. Although it is possible that some of the problem originates in incorrect treatment of conformational isomerism, it seems more likely that this relatively poor performance of theory reflects an inadequate treatment of the interplay between changes in the ionization and electron attachment energies on the one hand and changes in the solvation energies on the other hand, as one goes from the dimers to the monomer. Table 3 shows that the calculated increase in the ionization potential and in the electron attachment energy upon going to the less conjugated monomer **1** is ∼0.7 eV, and this is counteracted by a 0.4−0.5 eV gain in solvation energy of the smaller ions from **1**. In reality, the two opposing quantities approximately cancel and the redox potentials of the dimers are very similar to those of the monomer. It is not clear which of the opposing quantities is calculated incorrectly, or if both are. The situation contrasts with our previous more satisfactory experience with the oxidation of a series of anions that were all of comparable size and showed no conformational isomerism[26,31] and provides a cautionary note for future calculations of redox potentials of series of species that differ significantly in size. At the same time, it provides a good test case for the development of better theoretical procedures.

Oxidation and Reduction of 10. This compound is 0.2 V easier to reversibly oxidize or to reduce than the monomer **1**. The calculated differences are again too large, 0.4 V for oxidation and 0.3 V for reduction. This double isobenzofuran exhibits a peculiar behavior upon cycling, and we plan to examine it more thoroughly.

EXPERIMENTAL PART AND COMPUTATIONAL DETAILS

Electrochemistry. *Materials.* Tetra-*n*-butylammonium hexafluorophosphate obtained from Fluka AG (>98%) was recrystallized twice from ethanol, dried in a vacuum oven, and kept in a vacuum desiccator over P_2O_5. Anhydrous SO_2 gas (99.98%) obtained from Linde Technoplyn, Prague, Czech Republic, was condensed at −70 °C in a dried flask and purified by stirring magnetically for 30 min with highly activated alumina (basic type 5016A, Fluka AG). *N*,*N*-Dimethylformamide (DMF), purchased from Fluka absolute (>99.8%), was purified by azeotropic distillation with 5% water and 5% benzene followed by vacuum fractionation under argon atmosphere.[32]

Measurements. All voltammetric measurements were performed using an AUTOLAB potentiostat (PGSTAT30) controlled by a PC with GPES software. Direct current polarography was recorded using an analog potentiostat PA3 connected with an XY recorder (Laboratorní Přístroje Praha), the controlled drop time was 2 s, and a typical scan rate was 10 mV/s at the sensitivity of 50 nA/cm. The supporting electrolytes were 0.1 M $[NBu_4][PF_6]$ and $[NOct_4][ClO_4]$.

Cyclic voltammetric measurements in liquid SO_2 were carried out in a single-compartment glass cell using a Pt disk (1.0 mm diameter) working electrode, a Pt plate counter electrode, and an Ag rod as a quasireference electrode. Ferrocene (Fc^+/Fc) was used (0.3−0.5 mM) as an internal reference. The volume of the five-neck conical shaped electrochemical cell was ∼10 mL. The cell containing enough substrate, electrolyte, and ferrocene, along with a magnetic stirrer, was placed on the vacuum line (7.0 mbar) and then filled and evacuated with argon several times. Purified SO_2 was distilled into the cell at −70 °C to prepare a submilimolar solution (∼4 mL), and the measurements were performed at the same temperature and above, up to 22 °C, at scan rates typically ranging 0.08−5.0 V/s under argon atmosphere.

In DMF, cyclic voltammetric and polarographic reduction experiments were carried out using a hanging mercury drop working electrode (HMDE), a Pt plate counter electrode, and a saturated calomel electrode (SCE) with a nonaqueous salt bridge as a reference electrode at room temperature, while for oxidation experiments the Pt disk was used as the working electrode. Submillimolar solutions were prepared by dissolving the dimer in DMF (8 mL), and the measurements were performed under Ar atmosphere after several minutes of deaeration. The scan rates of CVs were from 0.1 to 5.0 V/s. The reproducibility of potential measurements was ±5 mV.

Computational Details. Quantum chemical calculations were performed using the TURBOMOLE 6.4 program. Geometry optimizations were carried out in the RI-DFT-PBE[33] approximation.[34] During the optimization, the def2-SVP basis set was employed on all atoms,[35] whereas the def2-TZVP basis set was used for the final single-point calculations to obtain molecular energies.[36] For all open-shell systems, the unrestricted Kohn−Sham (UKS) formalism was used. The addition of an empirical dispersion term to the DFT calculations (DFT+D3[37]) changed the calculated reduction potentials by less than 0.01 V, and those values are not reported.

dx.doi.org/10.1021/jo502004r | J. Org. Chem. 2015, 80, 80−89

Solvation effects were taken into account by using the COSMO-RS (conductor-like screening model for realistic solvation) method.[38,39] The standard COSMO calculations[40] required by the COSMO-RS protocol were carried out employing the TURBOMOLE 6.4 program. The recommended protocol involving the Becke−Perdew (B−P) functional[41−43] for the vacuum and the $\varepsilon_r = \infty$ (ideal screening) calculations (at the $\varepsilon_r = x$ optimized geometries, where x is the dielectric constant of the solvent) together with the def-TZVP basis set was used. Final COSMO-RS calculations were carried out using the COSMO*therm*[44] program.

The Gibbs free energy and reduction potentials were calculated from

$$G = E_{el} + \Delta G_{solv} + E_{ZPVE} + pV - RT \ln(q_{trans}q_{rot}q_{vib}) \quad (1)$$

$$E^0/V = 27.21(G_{ox}/\text{au} - G_{red}/\text{au}) - E^0{}_{abs}(\text{NHE})/\text{V} \quad (2)$$

where E_{el} is the vacuum energy of the system (RI-PBE/def2-TZVP//RI-PBE/def2-SVP) and G_{solv} is the solvation free energy (from RI-BP/def-TZVP,COSMO-RS, $\varepsilon = 1$, $\varepsilon = \infty$). E_{ZPVE} is the zero-point energy, and $pV - RT \ln(q_{trans}q_{rot}q_{vib})$ accounts for thermal corrections to the enthalpy and entropy terms, obtained from a frequency calculation with the procedure used for the geometry optimization (RI-PBE/def2-SVP level), at 298 K and 1 atm using the ideal gas approximation. $G_{ox/red}$ is the Gibbs free energy of the oxidized (reduced) form and the $E^0{}_{abs}$(NHE) is the absolute potential of the normal hydrogen electrode (NHE). The latest value[27] $E^0{}_{abs}$(NHE) = 4.281 V was used.

Synthesis. *General Information.* All reagents were commercially available and were used without further purification unless otherwise noted. All reactions were monitored by TLC with GF254 silica gel coated plates. Flash column chromatography was carried out by using 200−300 mesh silica gel at increased pressure. ^{1}H NMR and ^{13}C NMR spectra were recorded with a 400 MHz spectrometer in $CDCl_3$ solutions using tetramethylsilane as the internal standard unless stated otherwise. δ values are given in ppm and coupling constants (J) in Hz. Melting points were measured on a melting point apparatus and are uncorrected. IR spectra were recorded in KBr pellets, and ESI TOF was used to obtain HRMS.

Dimer Synthesis: General Procedure. To a solution of a dibromo compound (1 mmol) in THF (10 mL) at −78 °C was added 1.6 M BuLi in hexanes (3 mmol). The mixture was stirred at −78 °C for 10 min under Ar atmosphere and cannulated into a solution of 3-phenylphtalide (**11**, 3 mmol) in THF (10 mL). The red mixture was stirred at room temperature for 10 min and then at reflux temperature for another 30 min. It was cooled to rt, 5% aqueous HCl (20 mL) was added, and the mixture was extracted with ether. The ether phase was dried with $MgSO_4$, the solvent was evaporated, and the residue purified as stated below.

*Bis(p,p′-1,3-diphenylisobenzofuran) (**4**).* Compound **4** was purified by recrystallization from boiling DMSO to yield very fine red needlelike crystals (1.42 g, 82%), mp 297−298 °C. The compound is not stable in the presence of light and air; it reacts with oxygen to form an oxidized form of **4**. The oxidized form is more soluble in dichloromethane than is the parent compound. Therefore, this compound was dissolved in dichloromethane and filtered to remove the impurities from the crystallized pure compound under inert conditions. Alternatively, we also ran continuous Soxhlet extraction with dichloromethane. ^{1}H NMR (600 MHz, CD_2Cl_2): δ 8.10 (d, J = 8.2, 4H), 8.01 (d, J = 8.2, 4H), 7.92 (ddd, J = 2.4, 5.5, 9.4, 4H), 7.86 (d, J = 8.2, 4H), 7.52 (dd, J = 5.7, 9.6, 4H), 7.33 (dd, J = 4.1, 11.4, 2H), 7.16−7.03 (m, 4H). ^{13}C NMR (201 MHz, CD_2Cl_2): δ 144.51, 144.02, 139.01, 132.08, 131.17, 129.55, 127.72, 127.60, 125.98, 125.91, 125.59, 125.32, 122.99, 122.82, 120.75, 120.74. IR (KBr): ν 3020 (w), 1589 (s), 1484 (s), 1442 (m), 1203 (s) cm^{-1}. HRMS (ESI+): calcd for $C_{40}H_{27}O_2^+$ (M + H$^+$) 539.2011, found 539.2015. Anal. Calcd for $C_{40}H_{26}O_2$: C 87.73, H 4.97. Found: C 87.83, H 4.73.

*3,3′-(Biphenyl-3,4′-diyl)bis(1-phenylisobenzofuran) (**5**).* Compound **5** was recrystallized from an acetone-methanol mixture (1:10) as a yellow solid (80% yield). Mp: 198−199 °C. ^{1}H NMR (400 MHz, CD_2Cl_2): δ 8.31 (s, 1H), 8.16 (d, J = 8.5 Hz, 2H), 8.05 (d, J = 8.4 Hz, 4H), 8.04−7.93 (m, 5H), 7.92 (d, J = 8.4 Hz, 2H), 7.71−7.62 (m, 2H), 7.61−7.51 (m, 4H), 7.38 (td, J = 7.5, 1.0 Hz, 2H), 7.21−7.08 (m, 4H). ^{13}C NMR (101 MHz, CD_2Cl_2): δ 144.16, 143.76, 141.39, 139.24, 132.34, 131.71, 131.01, 129.75, 129.19, 127.84, 127.25, 125.64, 125.54, 125.51, 125.22, 124.99, 124.97, 123.92, 123.23, 122.63, 122.55, 122.43, 122.34, 120.39, 120.32. IR (KBr): ν (cm^{-1}) 3050 (w), 1600 (s), 1470 (m), 1320 (m), 1200 (m). MS (ESI+): calcd for $[C_{40}H_{26}O_2Li]^+$ 545.2088, found 545.2101.

*3,3′-Bis(3-phenylisobenzofuran-1-yl)biphenyl (**6**).* Compound **6** was recrystallized from an acetone−methanol mixture (1:10) as a yellow solid (92% yield). Mp: 203−205 °C. ^{1}H NMR (400 MHz, CD_2Cl_2): δ 8.31 (m, 2H), 8.02 (m, 4.0 Hz, 1H), 7.98 (m, 2H), 7.92 (m, 2H), 7.67 (m, 4H), 7.52 (m, 4H), 7.34(m, 2H), 7.11(m, 4H). ^{13}C NMR (101 MHz, CD_2Cl_2): δ 144.19, 143.75, 141.94, 132.34, 131.70, 129.76, 129.20, 127.26, 126.00, 125.68, 125.54, 124.98, 124.07, 123.66, 122.62, 122.34, 120.40, 120.29. IR (KBr): ν (cm^{-1}) 3023 (w), 1597 (s), 1460 (m), 1307 (s), 1190 (s). MS (ESI+): calcd for $[C_{40}H_{26}O_2Li]^+$ 545.2088, found 545.2075.

*1,2-Bis[4-(3-phenylisobenzofuran-1-yl)phenyl]ethane (**7**).* Compound **7** was recrystallized from methanol (85% yield). Mp: >230 dec. ^{1}H NMR (400 MHz): δ 7.95 (d, 4H, J = 7.5 Hz), 7.88 (d, 4H, J = 7.5 Hz), 7.84 (m, 4H), 7.49 (t, 4H, J = 7.51 Hz), 7.30 (m, 6H), 7.02 (m, 4H), 3.03 (s, 4H). ^{13}C NMR (75 MHz): δ 144.1, 143.6, 140.7, 132.0, 130.0, 129.4, 129.2, 127.0, 125.1, 125.0, 122.3, 122.0, 120.6, 37.9. IR: ν 3040 (w), 2900 (w), 1590 (s) cm^{-1}. MS (ESI+): calcd for $[C_{42}H_{30}O_2Li]^+$ 573.2401, found 573.2415.

*1,3-Bis(4-(3-phenylisobenzofuran-1-yl)phenyl)propane (**8**).* Compound **8** was recrystallized from methanol (80% yield). Mp: 150 °C. ^{1}H NMR (400 MHz): δ 7.95 (d, 4H, J = 7.5 Hz), 7.88 (d, 4H, J = 7.5 Hz), 7.84 (m, 4H), 7.49 (t, 4H, J = 7.51 Hz), 7.30 (m, 6H), 7.02 (m, 4H), 2.75 (t, 4H, J = 7.51 Hz), 2.06 (m, 2H). ^{13}C NMR (75 MHz): δ 144.3, 143.6, 141.4, 132.0, 129.6, 129.3, 129.1, 127.0, 125.4, 125.1, 124.9, 122.3, 122.0, 120.5, 120.4, 35.4, 33.0. IR (KBr): ν 3050 (w), 2950 (w), 1590 (s) cm^{-1}. MS (ESI+): calcd for $[C_{43}H_{32}O_2Li]^+$ 587.2557, found 587.2566.

*1-Phenyl-3-(3-(3-(4-(3-phenylisobenzofuran-1-yl)phenyl)propyl)-phenyl)isobenzofuran (**9**).* Compound **9** was recrystallized from methanol (yield 80%). Mp: 130 °C. ^{1}H NMR (400 MHz): δ 7.96 (m, 4H), 7.89 (d, 2H, J = 8.43 Hz), 7.83 (m, 6H), 7.49 (dt, 4H, J = 2.02, 8.06 Hz), 7.43 (t, 1H, J = 7.88 Hz), 7.35 (d, 2H, J = 8.24 Hz), 7.17 (d, 1H, J = 7.69 Hz), 7.02 (m, 4H), 2.79 (m, 4H), 2.11 (m, 2H). ^{13}C NMR (75 MHz): δ 144.2, 143.1, 141.4, 132.0, 131.9, 129.6, 129.4, 129.1, 127.4, 127.1, 127.0, 126.0, 126.4, 125.4, 125.1, 125.0, 124.9, 122.7, 122.3, 122.0, 120.5, 120.4, 120.3, 35.7, 35.4, 33.0. IR (KBr): ν 3050 (w), 2950 (w), 2870 (w), 1590 (s) cm^{-1}. MS (ESI+): calcd for $[C_{43}H_{32}O_2Li]^+$ 587.2557, found 587.2565.

*1,4-Bis(3-phenylisobenzofuran-1-yl)benzene (**10**).* To a solution of 1-(4-bromophenyl)-3-phenylisobenzofuran[22] (1.2 mmol) in dry THF (20 mL) at −78 °C was added 1.6 M *n*-BuLi in hexanes (1.6 mmol). The mixture was stirred at −50 °C under Ar atmosphere. After 1.5 h, 3-phenylphthalide (**11**, 1.6 mmol) was added and the reaction mixture was maintained at −50 °C under Ar atmosphere for 2 h. The red mixture was allowed to warm to room temperature overnight and HCl (36%, 2.5 mL) was added. After stirring 1 h more, diethyl ether (15 mL) was added and the organic phase was separated. More diethyl ether (50 mL) was added and the mixture was left resting for 1 h in the dark. The resulting solid was filtered and dried in the dark to give 105 mg of a bright red solid. Yield: 19%. Mp: 221−222 °C. ^{1}H NMR (THF-d_8, 400 MHz): δ 8.14 (s, 4H), 8.05−7.95 (m, 8H), 7.52−7.48 (t, J = 7.8 Hz, 4H), 7.32−7.28 (t, J = 7.5 Hz, 2H), 7.11−7.06 (m, 4H). ^{13}C NMR (THF-d_8, 101 MHz): δ 143.84, 143.37, 131.45, 129.61, 128.77, 126.78, 125.31, 125.24, 124.74, 124.53, 122.53, 122.36, 120.08. IR: ν 3092 (w), 3055 (w), 1625 (s), 1597 (m), 1500 (s), 1390 (m), 1212 (m), 1115 (m), 999 (m) cm^{-1}. MS (ESI+): calcd for $C_{34}H_{23}O_2^+$ (MH^+) 463.1698, found 463.1720. Anal. Calcd for $C_{34}H_{22}O_2$: C, 88.29; H, 4.79. Found: C, 88.42; H, 5.15.

*1-(3-Bromophenyl)-3-(4-bromophenyl)propane (**13**).* (*E*)-3-(3-Bromophenyl)-1-(4-bromophenyl)prop-2-en-1-one (**12**) was prepared by a modified literature procedure.[18] To a mixture of 4-bromoacetophenone (2.2 g, 11 mmol) and 3-bromobenzaldehyde (2

dx.doi.org/10.1021/jo502004r | J. Org. Chem. 2015, 80, 80−89

g, 11 mmol) in ethanol (50 mL) was added a solution of NaOH (0.66 g) in water (15 mL). The mixture was stirred for 30 min. A light yellow solid **12** formed and was collected by filtration (3.9 g, 97%). ^{1}H NMR (300 MHz): δ 7.89 (d, 2H, J = 8.46 Hz), 7.79 (t, 1H, J = 1.71 Hz), 7.73 (d, 1H, J = 15.7 Hz), 7.66 (d, 2H, J = 8.34 Hz), 7.54 (m, 2H), 7.46 (d, 1H, J = 15.66 Hz), 7.30 (t, 1H, J = 7.83 Hz). A solution of **12** (3.32 g, 9 mmol) in trifluoroacetic acid (30 mL) containing triethylsilane (9 mL) was stirred for 30 min and quenched with water (100 mL). The product was extracted with dichloromethane to give 2.80 g (88% yield) of **13** as viscous oil. ^{1}H NMR (300 MHz): δ 7.41 (d, 2H, J = 5.1 Hz), 7.33 (m, 2H), 7.162 (t, 1H, J = 4.5 Hz), 7.1 (d, 1H, J = 4.5), 7.06 (d, 2H, J = 5.1 Hz). ^{13}C NMR (75 MHz): δ 144.3, 140.8, 131.5, 131.4, 130.2, 129.9, 129.0, 127.1, 122.4, 119.6, 34.9, 34.7, 32.5. MS (ESI−): calcd for $[C_{15}H_{14}Br_2Cl]^-$ 388.9135, found 388.9147.

1,3-Bis(4-bromophenyl)propane (15). (*E*)-1,3-Bis(4-bromophenyl)prop-2-en-1-one (**14**) was prepared by a modified literature procedure.[18,19] To a mixture of 4-bromoacetophenone (2.2 g, 0.011 mol) and 4-bromobenzaldehyde (2 g, 0.011 mol) in ethanol (50 mL) was added a solution of NaOH (0.66 g) in water (15 mL). The mixture was stirred for 30 min while a light yellow solid product **14** formed. Filtration yielded 3.8 g (94% yield). ^{1}H NMR (300 MHz): δ 7.9 (d, 2H, J = 8.7 Hz), 7.76 (d, 1H, J = 15.69 Hz), 7.67 (d, 2H, J = 8.7 Hz), 7.58 (d, 2H, J = 8.67 Hz), 7.52 (d, 2H, J = 8.58 Hz), 7.48 (d, 2H, J = 15.72 Hz). A solution of **14** (2.6 g, 7 mmol) was dissolved in a mixture of trifluoroacetic acid (~26 mL) and triethylsilane (10 mL), and the milky white mixture was stirred for 30 min. The reaction was quenched with water (100 mL) and the product was extracted with dichloromethane to give 2.13 g (85% yield) of **15** as a viscous oil. ^{1}H NMR (300 MHz): δ 7.42 (d, 4H, J = 8.49 Hz), 7.06 (d, 4H, J = 8.58 Hz), 2.60 (t, 4H, J = 7.56 Hz), 1.92 (m, 2H). ^{13}C NMR (300 MHz): δ 140.9, 131.4, 130.2, 119.6, 34.6, 32.6. MS (ESI−): calcd for $[C_{15}H_{14}Br_2Cl]^-$ 388.9135, found 388.9147.

3,4′-Dibromobiphenyl.[45−47] This compound was prepared from 3-amino-4′-bromobiphenyl, obtained from 4′-bromo-3-nitro-1,1′-biphenyl. ^{1}H NMR (400 MHz, $CDCl_3$): δ 8.41 (s, 1H), 8.25−8.17 (m, 1H), 7.86 (m, 1H), 7.62 (m, 3H), 7.49 (d, J = 8.5 Hz, 2H). It was synthesized as reported[20,48] except that 10% Pd/C was used instead of 5% Pd/C. To a solution of 4-bromo-3′-nitrobiphenyl (1.5 g, 5.4 mmol) in ethanol (100 mL) was added Sn (3 g) and concentrated aqueous HCl (25 mL). The mixture was refluxed for 6 h, cooled to room temperature, and made alkaline with a KOH solution (6 M). The mixture was extracted with dichloromethane (3 × 50 mL), and the combined organic phases were dried over Na_2SO_4. After filtration of drying agent, the solvent was evaporated to yield 3-amino-4′-bromobiphenyl (1.3 g, 96%). ^{1}H NMR (500 MHz, CD_2Cl_2): δ 7.57 (d, J = 8.5 Hz, 2H), 7.45 (d, J = 8.5 Hz, 2H), 7.26 (t, J = 7.8 Hz, 1H), 6.98 (m, 1H), 6.89 (t, J = 2 Hz, 1H), 6.73 (m, 1H), 3.78 (s, 2H). The amine was used in the next step without purification. A solution of 3-amino-4′-bromobiphenyl (1.3 g, 5.2 mmol) in 30% H_2SO_4 (30 mL) was cooled below 5 °C. An ice-cold solution of $NaNO_2$ (2.5 equiv) in water (10 mL) was added slowly and the mixture was stirred for 20 min. This solution was slowly added to a solution of CuBr (5 g) in 48% HBr (150 mL), precooled in an ice bath. After warming to room temperature, the mixture was stirred for 4 h at 60 °C, cooled to room temperature, and extracted with ether (3 × 50 mL). The combined ether phases were dried over $MgSO_4$ and filtered, and ether was evaporated. The crude material was purified by column chromatography (9:1 hexanes:ethyl acetate) to give the product (1.20 g, 74%) as an oil. ^{1}H NMR (400 MHz): δ 7.69 (t, J = 2.4 Hz, 1H), 7.58 (d, J = 11.2 Hz, 2H), 7.48 (m, 2H), 7.42 (d, J = 11.2 Hz, 2H), 7.32 (t, J = 10.4 Hz, 1H).

■ ASSOCIATED CONTENT

Supporting Information

Spectral characterization of new compounds, calculated energies and geometries of compounds **1**−**10**, and an enlarged view of the cyclic voltammogram of **4**. This material is available free of charge via the Internet at http://pubs.acs.org.

■ AUTHOR INFORMATION

Corresponding Authors

*Email: jiri.ludvik@jh-inst.cas.cz.

*Email: michl@eefus.colorado.edu.

Present Addresses

‖Department of Chemistry, Middle East Technical University, 06800 Ankara, Turkey.

⊥Department of Chemistry, University of Science and Technology Meghalaya, Killing Road, Baridua, Ninth Mile, Ri-Bhoi District, Mehalaya-793101, India.

Notes

The authors declare no competing financial interest.

■ ACKNOWLEDGMENTS

This material is based upon work supported by the U.S. Department of Energy, Office of Science, Office of Basic Energy Sciences, under Award Number DE-SC0007004. Work in Prague was supported by the AS CR, RVO 61388963 and 61388955, and by GACR grants 13-21704S and 14-31419S.

■ REFERENCES

(1) Howard, J. A.; Mendenhall, G. D. *Can. J. Chem.* **1975**, *53*, 2199−2201.

(2) Paci, I.; Johnson, J. C.; Chen, X.; Rana, G.; Popović, D.; David, D. E.; Nozik, A. J.; Ratner, M. A.; Michl, J. *J. Am. Chem. Soc.* **2006**, *128*, 16546−16553.

(3) Smith, M. B.; Michl, J. *Chem. Rev.* **2010**, *110*, 6891−6936.

(4) Smith, M. B.; Michl, J. *Annu. Rev. Phys. Chem.* **2013**, *64*, 361−386.

(5) Hanna, M.; Nozik, A. J. *J. Appl. Phys.* **2006**, *100*, 074510/1−074510/8.

(6) Johnson, J. C.; Nozik, A. J.; Michl, J. *J. Am. Chem. Soc.* **2010**, *132*, 16302−16303.

(7) Schrauben, J.; Ryerson, J.; Michl, J.; Johnson, J. *J. Am. Chem. Soc.* **2014**, *136*, 7363−7373.

(8) Ryerson, J.; Schrauben, J. N.; Ferguson, A. J.; Sahoo, S. C.; Naumov, P.; Havlas, Z.; Michl, J.; Nozik, A. J.; Johnson, J. C. *J. Phys. Chem. C* **2014**, *118*, 12121−12132.

(9) Greyson, E. C.; Stepp, B. R.; Chen, X.; Schwerin, A. F.; Paci, I.; Smith, M. B.; Akdag, A.; Johnson, J. C.; Nozik, A. J.; Michl, J.; Ratner, M. A. *J. Phys. Chem. B* **2010**, *114*, 14223−14232.

(10) Johnson, J. C.; Nozik, A. J.; Michl, J. *Acc. Chem. Res.* **2013**, *46*, 1290−1299.

(11) Schwerin, A. F.; Johnson, J. C.; Smith, M. B.; Sreearunothai, P.; Popović, D.; Černý, J.; Havlas, Z.; Paci, I.; Akdag, A.; MacLeod, M. K.; Chen, X.; David, D. E.; Ratner, M. A.; Miller, J. R.; Nozik, A. J.; Michl, J. *J. Phys. Chem. A* **2010**, *114*, 1457−1473.

(12) Müller, A. M.; Avlasevich, Y. A.; Müllen, K.; Bardeen, C. J. *Chem. Phys. Lett.* **2006**, *421*, 518−522.

(13) Burdett, J.; Müller, A. M.; Gosztola, D.; Bardeen, C. J. *J. Chem. Phys.* **2010**, *133*, 144506/1−12.

(14) Michl, J.; Nozik, A. J.; Chen, X.; Johnson, J. C.; Rana, G.; Akdag, A.; Schwerin, A. F. In *Organic Photovoltaics VIII*; Kafafi, Z. H. Lane, P. A., Eds.; Proceedings of SPIE Volume *6656*, 2007; pp 66560E1−E9.

(15) Johnson, J. C.; Akdag, A.; Zamadar, M.; Chen, X.; Schwerin, A. F.; Paci, I.; Smith, M. B.; Havlas, Z.; Miller, J. R.; Ratner, M. A.; Nozik, A. J.; Michl, J. *J. Phys. Chem. B* **2013**, *117*, 4680−4695.

(16) Demir, A. S.; Reis, O.; Emrullahoglu, M. *J. Org. Chem.* **2003**, *68*, 10130−10134.

(17) Liu, J.; Li, B. *Synth. Commun.* **2007**, *37*, 3273−3278.

(18) Patrick, D. A.; Bakunov, S. A.; Bakunova, S. M.; Kumar, E. V. K. S.; Lombardy, R. J.; Jones, S. K.; Bridges, A. S.; Zhirnov, O.; Hall, J. E.; Wenzler, T.; Brun, R.; Tidwell, R. R. *J. Med. Chem.* **2007**, *50*, 2468−2485.

(19) Chong, J. M.; Shen, L.; Taylor, N. J. *J. Am. Chem. Soc.* **2000**, *122*, 1822−1823.

(20) Doyle, M. P.; West, C. T. *J. Org. Chem.* **1975**, *40*, 3835−3838.

(21) Taylor, R. H.; Felpin, F.-X. *Org. Lett.* **2007**, *9*, 2911−2914.
(22) Kuninobu, Y.; Seiki, T.; Kanamaru, S.; Nishina, Y.; Takai, K. *Org. Lett.* **2010**, *12*, 5287−5289.
(23) Schrauben, J.; Akdag, A.; Wen, J.; Havlas, Z.; Johnson, J. C.; Michl, J. Unpublished results.
(24) Marenich, A. V.; Ho, J.; Coote, M. L.; Cramer, C. J.; Truhlar, D. G. *Phys. Chem. Chem. Phys.* **2014**, *16*, 15068−15106.
(25) Kelly, C. P.; Cramer, C. J.; Truhlar, D. G. *J. Phys. Chem. B* **2007**, *111*, 408−422.
(26) King, B. T.; Körbe, S.; Schreiber, P. J.; Clayton, J.; Němcová, A.; Havlas, Z.; Vyakaranam, K.; Fete, M. G.; Zharov, I.; Ceremuga, J.; Michl, J. *J. Am. Chem. Soc.* **2007**, *129*, 12960−12980.
(27) Isse, A. A.; Gennaro, A. *J. Phys. Chem. B* **2010**, *114*, 7894−7899.
(28) Namazian, M.; Lin, C. Y.; Coote, M. L. *J. Chem. Theory Comput.* **2010**, *6*, 2721−2725.
(29) Rokob, T. A.; Srnec, M.; Rulíšek, L. *Dalton Trans.* **2012**, *41*, 5754−5768.
(30) Khobragade, D. A.; Mahamulkar, S. D.; Pospíšil, L.; Císařová, I.; Rulíšek, L.; Jahn, U. *Chem.—Eur. J.* **2012**, *18*, 12267−12277.
(31) Wahab, A.; Stepp, B. R.; Douvris, C.; Valášek, M.; Šturša, J.; Klíma, J.; Piqueras, M.-C.; Crespo, R.; Ludvík, J.; Michl, J. *Inorg. Chem.* **2012**, *51*, 5128−5137.
(32) Liska, A.; Vojtisek, P.; Fry, A. J.; Ludvík, J. *J. Org. Chem.* **2013**, *78*, 10651−10656.
(33) Perdew, J. P.; Burke, K.; Ernzerhof, M. *Phys. Rev. Lett.* **1996**, *77*, 3865−3868.
(34) Eichkorn, K.; Treutler, O.; Öhm, H.; Häser, M.; Ahlrichs, R. *Chem. Phys. Lett.* **1995**, *240*, 283−290.
(35) Weigend, F.; Ahlrichs, R. *Phys. Chem. Chem. Phys.* **2005**, *7*, 3297−3305.
(36) Schäfer, A.; Huber, C.; Ahlrichs, R. *J. Chem. Phys.* **1994**, *100*, 5829−5835.
(37) Grimme, S.; Antony, J.; Ehrlich, S.; Krieg, H. *J. Chem. Phys.* **2010**, *132*, 154104−1−154104−9.
(38) Klamt, A. *J. Phys. Chem.* **1995**, *99*, 2224−2235.
(39) Klamt, A.; Jonas, V.; Buerger, T.; Lohrenz, J. C. W. *J. Phys. Chem. A* **1998**, *102*, 5074−5085.
(40) Klamt, A.; Schuurmann, G. *J. Chem. Soc., Perkin Trans. 2* **1993**, 799−805.
(41) Becke, A. D. *Phys. Rev. A* **1988**, *38*, 3098−3100.
(42) Vosko, S. H.; Wilk, L.; Nusair, M. *Can. J. Phys.* **1980**, *58*, 1200−1211.
(43) Perdew, J. P. *Phys. Rev. B* **1986**, *33*, 8822−8824.
(44) *COSMOtherm*, version C2.1, release 01.10. COSMOlogic GmbH & Co KG: Leverkusen, Germany.
(45) Case, F. H. *J. Am. Chem. Soc.* **1938**, *60*, 424−427.
(46) Broser, W.; Kurreck, H.; Niemeier, W.; Plato, M. *Tetrahedron* **1975**, *31*, 1769−1779.
(47) Leroux, F. R.; Bonnafoux, L.; Heiss, C.; Colobert, F.; Lanfranchi, D. A. *Adv. Synth. Catal.* **2007**, *349*, 2705−2713.
(48) Yeap, W. S.; Chen, S.; Loh, K. P. *Langmuir* **2009**, *25*, 185−191.